

Design and Control Analysis of an Automatic Active Domestic Solar Water Heating System

Leonard Akana Nguimdo*[‡] and Atanga Nelson Funue *

*Department of Electrical and Electronic Engineering, Faculty of Engineering and Technology, University of Buea, PO
Box 63 Buea, Cameroon

(languimdo@yahoo.fr, nelsonfunuea@yahoo.com)

[‡] Corresponding Author; L. Akana Nguimdo, PO Box 63 Buea, Tel: +237677975262, languimdo@yahoo.fr

Received: 16.11.2020 Accepted: 18.12.2020

Abstract- Solar water heating technology has become one of the most attractive methods of heating water in residential and public buildings with numerous benefits. This study presents the design technique for an automatic active domestic solar water heating system (ADSWHS) to satisfy the hot water demand for a residence in Wum (10.43°E, 6.23° N) with a daily hot water demand of 500 litres supplied at 70°C, using flat plate solar collectors and an arduino microcontroller. The solar data used in this analysis were obtained from Photovoltaic Geographical Information System (PVGIS) and the method used is the active direct roof mounted solar water heating. The system design process consist of evaluating the optimum collector tilt angle, the thermal analysis of the flat plate collector and hot water storage tank and finally modelling a low cost automatic controller for the system using a microcontroller in the Proteus software. The optimum annual average solar radiation on the tilted solar collector was obtained following the calculation of the conversion ratios of the direct, diffuse and reflected radiations. At annual time scale, the optimum tilt angle (β) that maximizes the collected radiation was 11° and the corresponding optimum average irradiance of 432 W/m² was obtained. The analytical results presented for the performance of the heater indicate that the system operates at an annual thermal efficiency of 55.49%. The control system simulation results indicate that the system uses 4.5kWh and 2.075kWh of energy to run the pump and the auxiliary heater respectively and produces 26.187kWh of energy to heat up the cold water from 25°C to 70°C for a single day.

Keywords Solar collectors, solar water heating, automatic controller, tilt angle, recirculation.

1. Introduction

Energy is a key factor for the development of our modern society as it plays a vital role in our daily activities. In general energy sources are grouped into two categories: non-renewable and renewable sources [1]. Non-renewable energy only available in limited amount is not replaced in a relatively short period of time while renewable energy is the form that is naturally replenished at human time scale [1] [2]. Current statistics reveals that 78.3% of the world energy consumption is stills obtained from fossil fuels while the rapid developing renewables accounts only for 19.1%. [3]. Renewable energy has become particularly attractive for decades now given the environmental consequences of fossil fuel and its limited amount compared to solar energy which is considered unlimited with respect to its potential in relation to the energy demand of humanity. Solar energy is

the most creditable renewable energy source that can be exploited in different ways, with the two most promising being photovoltaic and concentrated solar energy [4]. The sun radiates about 1.353 KW/m² of solar power at the top of the earth's atmosphere [5]. The use of this solar energy is an environmentally friendly solution that helps mitigate the deregulation of the earth/atmosphere system [6].

The direct utilization of solar energy for water heating in domestic applications is one of the most attractive methods of utilizing solar energy which is environmentally promising with regards to the problems posed by greenhouse gases [7]. Solar collectors are used for the optimal and efficient utilization of solar energy and their performance depends on the weather conditions, collector type and orientation [8] [9] [10]. Recent research works reveal that the domestic sector in the UK currently accounts for about one third of national

energy consumption and is responsible for over 25% of the total greenhouse gas emissions [11]. This is because domestic activities including space and water heating heavily rely on fossil fuels [12]. Moreover, water heating in most parts of the world is still based to a greater extent on natural gas which has a high CO₂ content and the rest supplied by electricity [12]. Hence, it becomes an imperious necessity to consider renewable energy sources in order to preserve our planet. In this context, the use of solar energy to heat water for domestic applications will greatly limit the emission of CO₂ and hence climate change.

Solar water heating technology is generally divided into two areas: The active and the passive systems [13]. Both systems use either direct or indirect heating [14]. Depending on the classical form of the radiation, conversion isn't enough to assure the optimum functioning of the heating systems [15]. Hence control system optimization approaches are of great importance [16] [17]. Several works have been published on multiple control optimization methods for solar water heating facilities [16]. Authors started by determining the optimal control strategy for water flow modulation in solar thermal applications using differential algorithm based on the ON/OFF principle as starter [18]. Thus the controller either starts or stops the pump according to the temperature difference. This control method is limited because it does not take care of other parameters like the level and the temperature of water inside the tank. Multiple control strategies nowadays exist for solar water heating systems and include Proportional-Integral-Derivative (PID) controllers, Proportional-Summation-Differentiation (PSD) controllers, and fuzzy logic controllers [19]. These methods may certainly be more practical in programming but are relatively complex and costly.

Today, Microcontroller based systems are widely used for monitoring physical parameters (temperature, pressure, humidity, etc.) and in particular parameters linked to solar energy applications [19]. Nevertheless, the developed

electronic devices differ from one work to another according to the specific requirement of every application [19]. In this paper, we study the optimization of the design analysis and control of an automatic active domestic solar water heating system (ADSWHS) using flat plate solar collectors and an Arduino based microcontroller that improves the system performance at a lower cost.

2. Materials and method

2.1. Details of the solar water heater

The automatic ADSWHS is made up of three main subsystems: An energy conversion unit which consists of a solar thermal flat plate collector, a hot water storage tank system equipped with an auxiliary electric heater and an Arduino based microcontroller subsystem. The control subsystem is made of several electronic components (timers, counters, analog to digital converters (ADC), registers, relays etc.) while the solar collector is made of copper tubes, insulating materials, coating materials, casing, and glazing.

The solar collector chosen for this design is the flat plate collector (FPC A32) and the method used is the active direct roof mounted. For the purpose of this work, a solar hot water system is designed for a family of 6 members in Wum (10.043°E, 6.23° N), a locality in the North West region of Cameroon to heat water from 25 °C to 70 °C. A daily hot water demand of 500 litres was estimated using 50 litres/Inhabitant a day and 100 litres for the kitchen. This load demand is multiplied by 1.2 before choosing a storage tank system to ensure a tolerance according to the Institute of Sustainable Technologies (AEE) sizing method. Figure 1 presents a proposed model for the system.

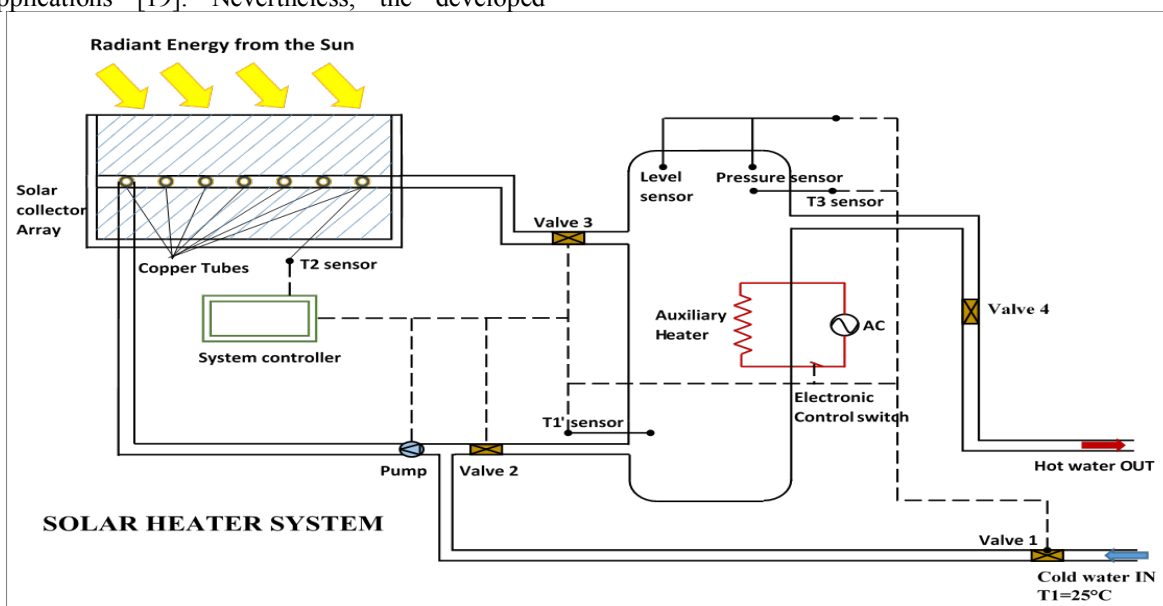


Fig. 1. Model for water circulation and heating

Cold water supplied at 25°C with the help of a pump undergoes forced circulation to the storage tank through the solar collector. The controller system uses four temperature sensors (T_1, T_1', T_2 and T_3), a pressure sensor and an ultrasonic sensor. T_1 measures the temperature of cold water that is pumped up to the solar collector during the normal operation loop (T_{in}), T_1' measures the temperature of the water entering the solar heater during a recirculation loop. T_2 measures the temperature of hot water from the collector (T_{out}) and T_3 measures the temperature of hot water inside the storage tank (T_{tank}). The ultrasonic sensor is used to measure the level of water inside the tank and gives information to the controller to stop the pumping of water to the collector when the tank is full. The pressure sensor is used to monitor the amount of pressure inside the tank for its safety.

To start the heating process, the temperature Delta T i.e. ($T_{out} - T_{in}$) must be equal or greater than 5 °C. This is to avoid activating the pump (water circulating) when there is not enough energy to be transferred. The temperature sensors are located at the solar collector fluid exit, the water supply inlet and at the bottom of the tank. This enables the controller to determine when to trigger the pump to transfer water from the tank to the solar collector.

An auxiliary electric heater is installed inside the hot water tank to take care of cases of poor irradiance. The activation of this electric heating device is automatically controlled by the microcontroller. The temperature sensor T_3 measures the temperature of hot water inside the tank (T_{tank}) in real time and sends an electric signal to the microcontroller. If this temperature is lower than the required

temperature value (70°C) and the solar radiation on the collector array is low ($\Delta T < 5^\circ\text{C}$), the microcontroller sets the electric heater "ON" automatically. When the required temperature is reached or the irradiance becomes important so as to satisfy Delta T condition, the controller disconnects the electric heater from the mains supply via an electronic controlled switch (Transistor).

2.2. Description of the solar data and system specifications

Wum (10.043°E, 6.23° N) receives on average a substantial annual solar energy of 5.3 kWh/m² or 424 W/ m² making it a suitable locality for the implementation of solar concentrating technology for water heating. The average daily solar data for Wum and system specification are given in tables 1 and 2 below.

Table 1. Average daily solar radiation intensity (E) for Wum [20]

Mo	Solar	Mo	Solar
Jan	6.3	Jul	4.3
Fe	6.4	Au	4.3
Ma	5.8	Sep	4.5
Ap	5.3	Oct	4.7
Ma	5.1	No	5.7
Jun	4.6	De	6.1
Average (E_{Mean})			5.3

Table 2. Specifications of the ADSWHS Design

Component	Specification	
Solar Collector	Type	FPC A32
	Length	/
	Width	/
	Area	2.98 m ²
	Tilt angle	11° (see below)
Absorber Sheet	Type	Black-painted aluminium
	Absorptivity	0.95 *0.96
	Transitivity	0.85*0.90
Glass Cover	Type	Hardened Glass (3.2 mm)
	Number	1
Storage Tank	Type	Thermally Insulated (500L)
	Auxiliary	1500W
Pump	Type	AC 220V, 6.5L/min

2.3. System design methodology

2.3.1. Solar radiation and optimum tilt angle (β)

The solar radiation I_T received by the inclined collector surface consists of three components: Direct radiation I_{b-T} , diffuse radiation I_{d-T} and the reflected radiation I_{r-T} [21]. Generally, available solar data is derived for local horizontal surface from which the components of solar radiation on the inclined are deduced through conversion.

The conversion is done for each component and thus, the total solar irradiance I_T received by the tilted surface is the sum of three terms given as

$$I_T = I_b R_b + I_d R_d + I_p R_r = I_b \frac{\cos\theta}{\cos\theta_z} + I_d \frac{1+\cos\beta}{2} + I_p \frac{1-\cos\beta}{2} \tag{1}$$

Where β , θ and θ_z are the tilt angle, solar incident angle and solar zenith angle respectively and ρ is the reflectance of the ground. I_b , I_d and I are direct, diffuse and global incident radiations on the horizontal surface at the location. R_b , R_d and R_r are conversion factors for direct, diffuse and reflected radiations respectively. The evaluation of the diffuse radiation component is based on the assumption of isotropic diffusion given by the Liu and Jordan's model [22]

Dividing Eq. (1) by I gives the total conversion factor linking the total irradiance on horizontal and that on inclined surface.

$$\frac{I_T}{I} = \left(1 - \frac{I_d}{I}\right) \frac{\cos\theta}{\cos\theta_z} + \frac{I_d}{I} \frac{1+\cos\beta}{2} + \rho \frac{1-\cos\beta}{2} \quad (2)$$

The ratio $\frac{I_d}{I}$ varies according to the clearness index (K) of the location [15] and is given as follows

$$\frac{I_d}{I} = \begin{cases} 1 - 0.09K & \text{for } K \leq 0.22 \\ 0.9511 - 0.1604K + 4.388K^2 - 16.638K^3 + 12.336K^4 & \text{for } 0.22 < K < 0.8 \\ 0.165 & \text{for } K \geq 0.8 \end{cases} \quad (3)$$

Where $K = \frac{I}{I_0}$ with $I_0 = 1367W/m^2$

The optimization technique applied here is therefore aimed at deriving the efficient tilt angle (β) for the locality that provides the highest collection efficiency of the collector through the year. The angles that correspond to the highest total conversion factor are first determined for each month. The solar irradiation data on horizontal surface used in this analysis are for the year 2016 and were obtained from Photovoltaic Geographical Information System (PVGIS) [23]. PVGIS is the official website of the European Union which makes available solar irradiation data, ambient temperature and tools for estimating the performance of photovoltaic systems. In this analysis, the characteristic parameters associated with mean solar days geometry as defined by Akana and Njomo [24] were taken into account and the single value of optimum tilt angle derived per month corresponds to the one that allows the maximum solar energy over the monthly mean solar day. Finally, the unique optimum angle to be applied to the system is identified as the monthly angle that provides the highest incident solar energy on the collector over the year.

2.3.2. Thermal analysis of flat plate solar collector

The amount of energy received by a tilted solar collector is given by

$$Q_c = I_T A_c \quad (4)$$

Where A_c is the area of the collector and I_T the incident irradiance on the tilted solar collector surface.

Part of this radiation is back-scattered to space and another portion absorbed by the glass cover. The fraction transmitted through the glass that is received by the absorber plate is thus

$$Q_{in} = I_T(\tau\alpha) \cdot A_c \quad (5)$$

The rate of heat loss (Q_{Loss}) depends on the collector overall heat loss coefficient (U_L) and the collector temperature.

$$Q_{Loss} = U_L A_c (T_c - T_a) \quad (6)$$

Thus, the rate of useful energy extracted by the collector (Q_u) is expressed as

$$Q_u = Q_{in} - Q_{Loss} = I_T(\tau\alpha) \cdot A_c - U_L A_c (T_c - T_a) \quad (7)$$

Where T_c and T_a are collector and ambient temperatures respectively. τ is the glass cover transmittance and α the absorptance of the absorber plate.

This useful energy delivered by the collector can also be given as

$$Q_u = \dot{m} C_p (T_{out} - T_{in}) \quad (8)$$

Where \dot{m} is mass flow rate of the fluid inside the collector in kg/s, C_p the specific heat capacity of water in kJ/kg.K. T_{in} and T_{out} are inlet and outlet fluid temperatures ($^{\circ}C$) respectively.

It is convenient to define the heat removal factor (F_R) as

$$F_R = \dot{m} C_p (T_{out} - T_{in}) / A_c [I_T(\tau\alpha) - U_L(T_{in} - T_a)] \quad (9)$$

The heater output temperature can therefore be expressed as

$$T_{out} = \frac{F_R A_c [I_T(\tau\alpha) - U_L(T_{in} - T_a)]}{\dot{m} C_p} + T_{in} \quad (10)$$

The maximum possible useful energy delivered by a flat plate solar collector is obtained in the case where the entire collector is at the inlet fluid temperature. The collector instantaneous thermal efficiency (η_c) is then defined as

$$\eta_c = F_R(\tau\alpha) - F_R U_L (T_{in} - T_a) / I_T \quad (11)$$

2.3.3. Hot water storage tank system and analysis

The energy assessment of the storage tank can then be given as

$$(M C_p)_s \frac{dT_s}{dt} = Q_{Ut} - Q_{out} - Q_{loss} \quad (12)$$

Where M is the mass of storage capacity (kg). Q_{Ut} is the heat delivered to the storage tank by the solar collector and Q_{out} the heat removed from storage tank to the load. The storage tank heat loss is given by

$$Q_{loss} = (UA)_s (T_s - T_a) \quad (13)$$

Where $(UA)_s$ is the storage tank heat loss capacity in (W/K) and T_a the ambient temperature.

To assess the long-term storage capacity of the tank, equation (12) may be rewritten as

$$T_{sn} = T_s + \frac{\Delta t}{(Mc_p)_s} [Q_{ut} - Q_{out} - (UA)_s (T_s - T_a)] \quad (14)$$

Where T_{sn} is the actual temperature inside the tank after time interval Δt .

In order to optimize the use of solar energy and limit the consumption of electrical energy, the heating procedure is planned such that the objective of obtaining 500 litres of water in the tank at 70°C is achieved before sunset. Therefore, the thermal efficiency that describes storage capacity of the tank is evaluated at the time when there is no heat transfer into or out of the tank. Equation (14) under these conditions reduces to

$$T_{sn} = T_s - \frac{\Delta t}{(Mc_p)_s} [(UA)_s (T_s - T_{env})] \quad (15)$$

The storage tank instantaneous efficiency η_s is then given by

$$\eta_s = \frac{T_s - \frac{\Delta t}{(Mc_p)_s} [(UA)_s (T_s - T_{env})]}{T_s} \quad (16)$$

The heat loss coefficient of the storage tank for this design is calculated according to the European standard for hot water storage tank systems (CEN/TC 228 2006 CEN/TC 228 WI 025) given by

$$(UA)_s = 0.16 V_{st}^{0.5} W/^\circ C \quad (17)$$

Where V_{st} is the volume of the hot water storage tank.

2.3.4. System controller components and design

Table 3 summarizes the characteristics of the controller components used in this design.

Table 3. Controller components

Component	Specification
Microcontroller	Arduino Uno
LCD display	A 2x16 LCD
Ultrasonic sensor	HC - SR04
Temperature	LM35 IC
Pressure sensor	MPX5500

The software program for the control system is developed using the arduino intergrated development invironment (IDE) software and the flow chart of the system is shown in Figure 2.

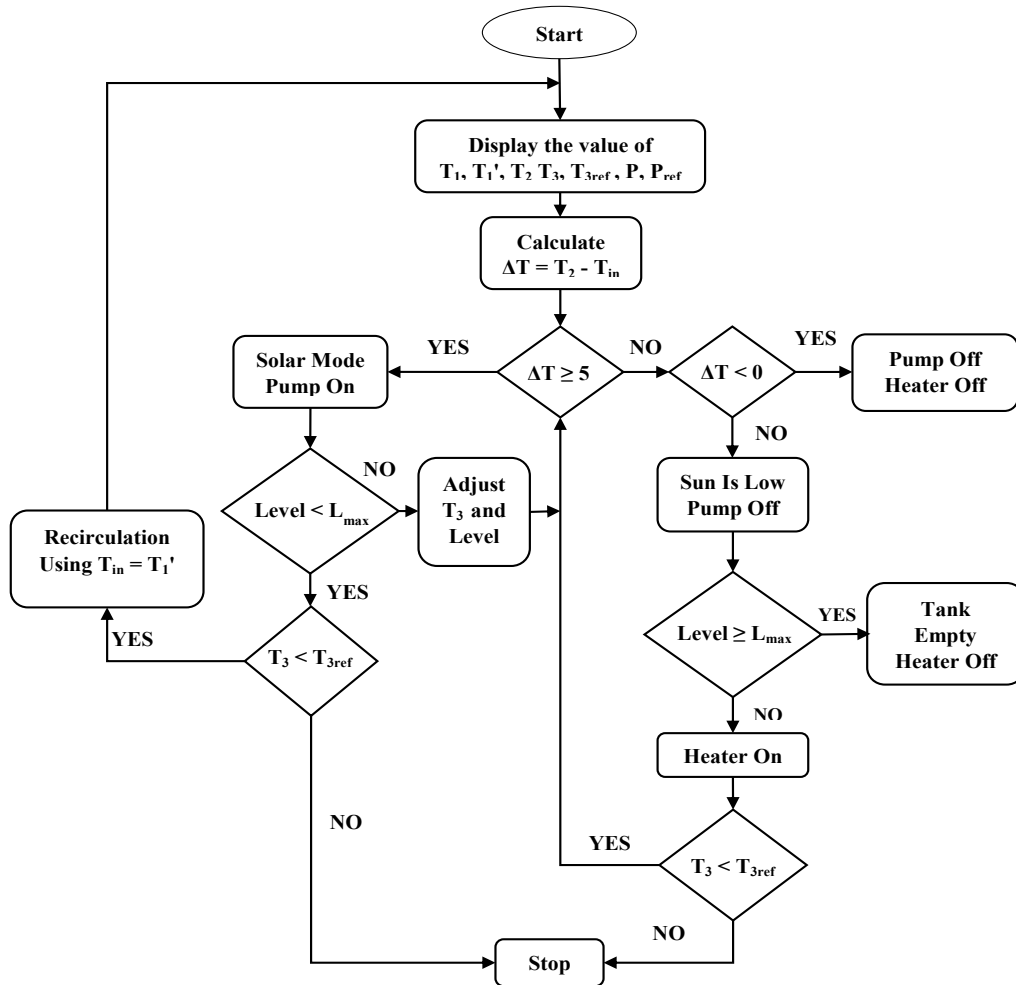


Fig. 2. Control system flow chart.

3. Results

3.1. Tilt angle analysis results

Figure 3 shows the variation of the total incident solar energy on the inclined surface at monthly time scale for the tilt angle ranging from 0° to 90°. The monthly optimum angle is then deduced as the one corresponding to the highest

value of the incident energy. From table 4 that summarizes these angles, it can be noted that this result is different from the latitude of the location often used by many researchers as the tilt angle. The corresponding daily incident energy for most of the cases is quite greater than the average obtained in Wum on horizontal surface. However, for the period expanding from April to August, the best surface remains the horizontal, a result which is still in accordance with past analysis [24].

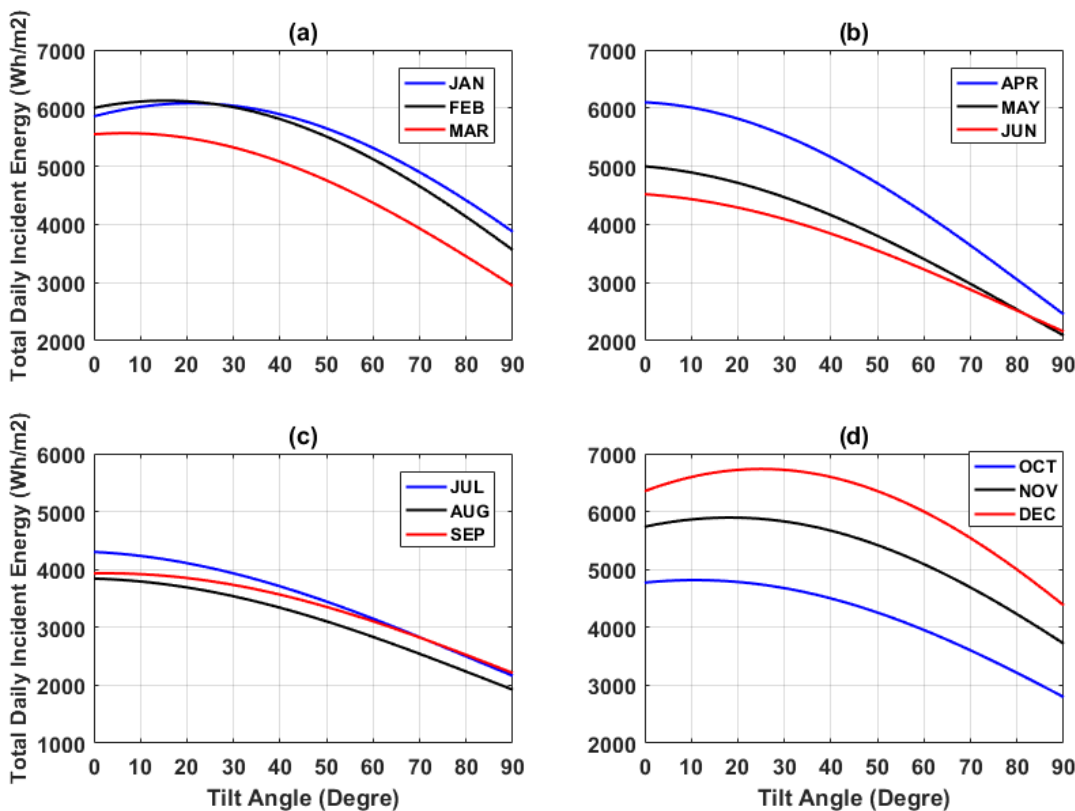


Fig. 3. Tilt angle analysis

Table 4. Incident solar energy on inclined and horizontal surfaces and optimum tilt angles

	JAN	FEB	MAR	APR	MAY	JUN	JUL	AUG	SEP	OCT	NOV	DEC
Optimum Tilt Angle (Degree)	21	15	7	0	0	0	0	0	3	11	19	25
Incident energy on horizontal (KWh/m²)	5.857	6.003	5.549	6.099	4.998	4.519	4.303	3.843	3.932	4.773	5.737	6.352
Incident energy on Incline (KWh/m²)	6.082	6.128	5.568	6.099	4.998	5.519	4.303	3.843	3.934	4.816	5.895	6.735

Evaluating the total annual incident solar energy based on the optimum tilt angles obtained at monthly time scale, a maximum of 64820 Wh/m² was obtained with a tilt angle of 11° while 63600 Wh/m² was measured on the horizontal. From these figures, it can be observed that the annual average irradiance obtained for a tilt angle of 11° is 432

W/m², which is greater than that on horizontal. Therefore 11° is the optimum tilt angle for the locality.

3.2. Flat plate solar collector and storage tank performances

The thermophysical parameters of the flat plate solar collector used in this analysis are defined as in Odigwe et al. [25]. Because a single layer glazing is used, τ is assumed 0.9. Likewise, U_L is estimated at $5.5\text{W/m}^2\text{K}$ and α is 0.96 given that black paint is applied on the collector fin plates. F_R is chosen to be 0.96 in accordance with Malvi et al. [26]. T_a is estimated at 23°C base on the site measurements during the research period. The performances of the solar collector using the input temperature as parameter are given in figure 4.

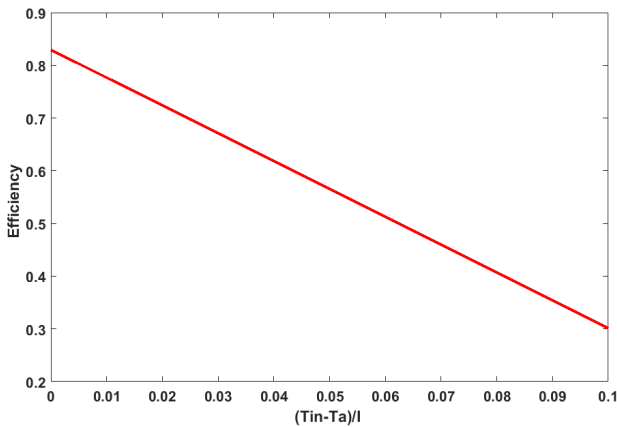


Fig. 4. Efficiency of a flat-plate collector at $T_a = 23^\circ\text{C}$

The efficiency is a linear function of the ratio $(T_{in} - T_a)/I_T$ supposing that F_R , τ , α , and U_L are constant for the solar collector under investigation. This leads to a straight line plot as shown on figure 4 with a slope of $(-F_R U_L)$. The maximum collector efficiency of 82.94% occurs when $T_{in} = T_a$. This maximum is essentially a function of optical and thermophysical properties of the collector. The efficiency reduces as $T_{in} - T_a$ increases. This is characterized by the fact that the amount of heat collected by water reduces as it passes through the collector when the input temperature increases. The efficiency at $T_{in} = 25^\circ\text{C}$ is 80.49% and decreases further for $T_{in} = 30^\circ\text{C}$ as shown on figure 4.

As far as the hot water storage tank is concerned, the following data for the calculation of the efficiency were used:

The time interval ranges from 6 pm to 6 am and corresponds to the night period in the locality ($\Delta t = 12$ hours). Also, $M = 500\text{Kg}$ or 0.5m^3 of water, $T_s = 70^\circ\text{C}$, $T_a = 23^\circ\text{C}$. By substituting V_{st} in equation (17) we obtain $(UA)_s = 0.113\text{W}/^\circ\text{C}$. Equation (16) then gives $\eta_s = 99.89\%$.

3.3. Sizing of the solar system

The useful energy yield (E_c) per m^2 of solar collector is

$$E_c = E_T \cdot \eta_c \cdot \eta_s = 4.342 \text{ kWh/m}^2 \cdot \text{day} \quad (18)$$

Where E_T is the average daily solar radiation intensity on the collector tilted surface.

The total area of solar collector array (C_A) is calculated as

$$C_A = Q_s/E_c = (26.188\text{KWh/day})/(4.341 \text{ kWh/m}^2 \cdot \text{day}) = 6.03 \text{ m}^2 \quad (19)$$

Q_s is the total energy required to heat the 500L of water.

Therefore the number of flat plate solar collectors base on the specifications of table 2 equals $N_c = \frac{C_A}{A_c} = 2.024$

From these calculations, two solar collectors connected in series configuration are needed for the design. This moderate number of collectors is because the system controller is able to recirculate the water to meet the required temperature of 70°C . The thermal efficiency of the series collector at a constant flow rate of 0.108Kg/s is given as

$$\eta_{cs} = F_R (\tau\alpha)_{series} - (F_R U_L)_{series} (T_{in} - T_a) / I_T \quad (20)$$

$$\eta_{cs} = 0.8154 - [5.191\text{W/m}^2(25 - 23)]/432 \text{ W/m}^2$$

$$\eta_{cs} = 79.136\%$$

The efficiency of the solar collector array (η_{Array}) is then given as

$$\eta_{Array} = \eta_c \times \eta_{cs} = 63.625\% \quad (21)$$

The system overall efficiency η_{system} is given as

$$\eta_{system} = \eta_{Array} \cdot \eta_s = 63.55\% \quad (22)$$

3.4. Control system simulations

The control system results presented on figure 5 were obtained using Wum hourly solar radiation for January from PVGIS [16]. Here, the simulation period considered is 24hours (one day) starting from midnight and (T_{in}) was set at 25°C at start. During this time period, the microcontroller calculates (T_{out}) according to equation (10). From figure 5(a), we noticed that the irradiance is zero from midnight to 6am. During this period, the pump and the auxiliary electric heater are off and the temperature difference Delta T (figure 5.b) is zero. This is normal since there is no solar energy to heat the water if it circulates. Also, the system is aimed at using the maximum energy from the sun since heating using electricity is more costly. The consequence therefore is that no water flows into the tank (figure 5.d). Between 6am and 7am, Delta T increases but remains below 5°C and the control system keeps the pump and heater off. As the irradiance increases with time, the temperature at the collector also increases. This leads to a corresponding rise of Delta T. Since there is enough energy to heat the water, the system triggers the pump for circulating the water. This is noticed as from 7am where T_{tank} increases significantly. Because of the high values of irradiance (figure 5a), the pump is ON until 14:00 and alternates with the heater as the irradiance drops in the afternoon. This alternating ON/OFF of the pump and heater generates the continuum that is recorded in the morning from 07:00 to 08:00 and 14:00 to 15:00 in the afternoon. The

continuum operation sequence is illustrated in the magnified form in figure 6 for the period ranging from 7am to 8am.

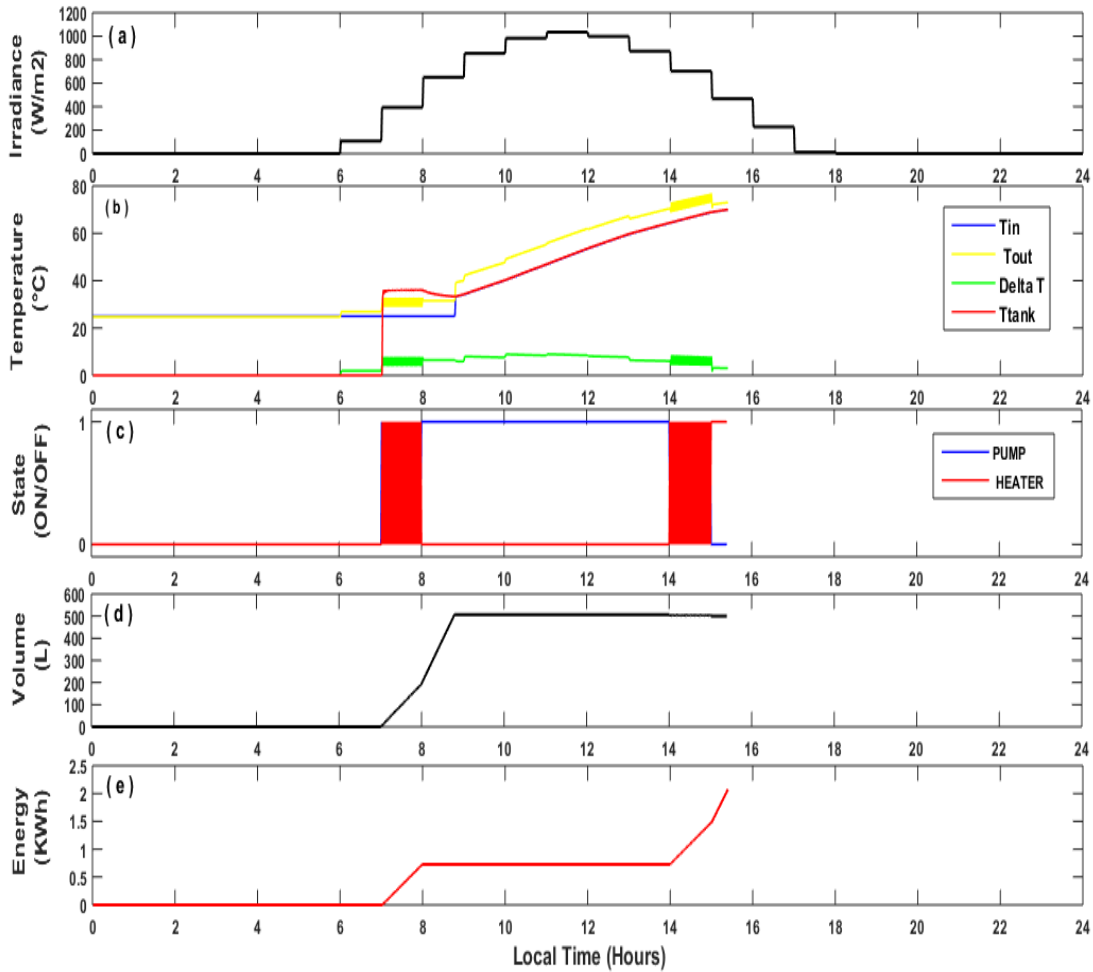


Fig. 5. Control system simulation results for 24 hours starting from midnight.

The maximum value of Delta T for the given data set is 8.6 °C. Since the required output temperature of hot water is 70 °C, the microcontroller is programmed to recirculate the water to meet this temperature. Due to the circulation of water at a flow rate of 6.5L per minutes, the tank gets full (figure 5.d) within a period of 77minutes but at very low temperature (figure 5.b). From that point, the control system activates the recirculation mode. The water now flows from the tank and it can be noticed from figure 5.b that $T_{in} = T_{tank}$ when the recirculation starts by 9 am. Figure 5(c) also shows

that when the controller triggers the pump at 8am, it remains ON until 2pm and during this interval, the hot water in the tank is being recirculated. The system stops when the tank is full with water at 70°C. This result is obtained for a typical day in Wum by 3:30pm as shown in figure 5(d). The variation of energy delivered to the system by the auxiliary heater for a day is presented on figure 5(e). It is seen that the heater delivers 2.075 kWh of energy to the system. This amount is far less than the 26.188 kWh needed to heat 500L of water from 25°C to 70°C.

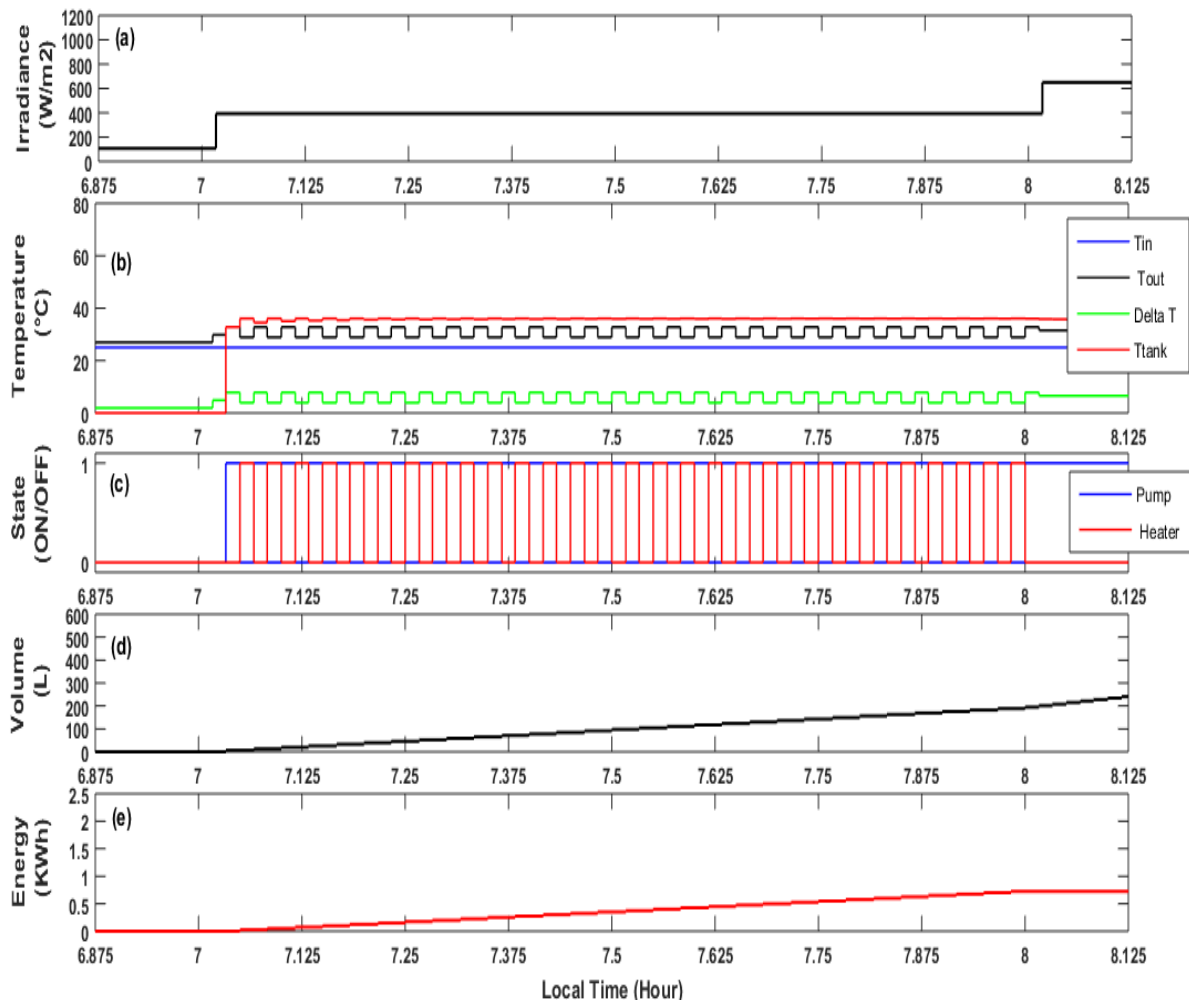


Fig. 6. Control system simulation results magnified from 7am and 8am

Figure 6 is a magnified representation of the control system activities from 7am to 8am. On this figure, the continuum shown on figure 5 for the above time interval has been expanded. It can be noticed from figure 6(b) that T_{in} remains constant during this interval. This is because the storage tank is not full and there is no recirculation yet. However, T_{out} varies but the amount of solar energy available does not allow Delta T to remain above 5°C. Since the control system detects that there is not enough energy from the sun, it triggers automatically the auxiliary heater which remains on until Delta T becomes once more greater than 5°C to trigger the pump. Figure 6(c) presents the ON/OFF state of the pump and the auxiliary heater for this time period. The results show that the microcontroller triggers both the pump and the heater thirty times each with each running for one minute. The volume of water inside the tank

and the amount of energy supplied to the system by the auxiliary heater during this period are 195L and 0.725KWh respectively as indicated on figures 6(d) and 6(e).

3.5. Importance of appropriate surface sizing

From the previous analysis, it is observed that the household need (500L at 70°C) is satisfied early enough before sunset. One may be tempted to reduce the size of solar array in order to reduce the cost. In this case, a good compromise should be found between the cost of the solar heater and the extra electric energy used by the auxiliary heater to assure the 70°C needed. Figure 7 shows the system performances when the total surface of the panels undergoes 0.46 m² reduction.

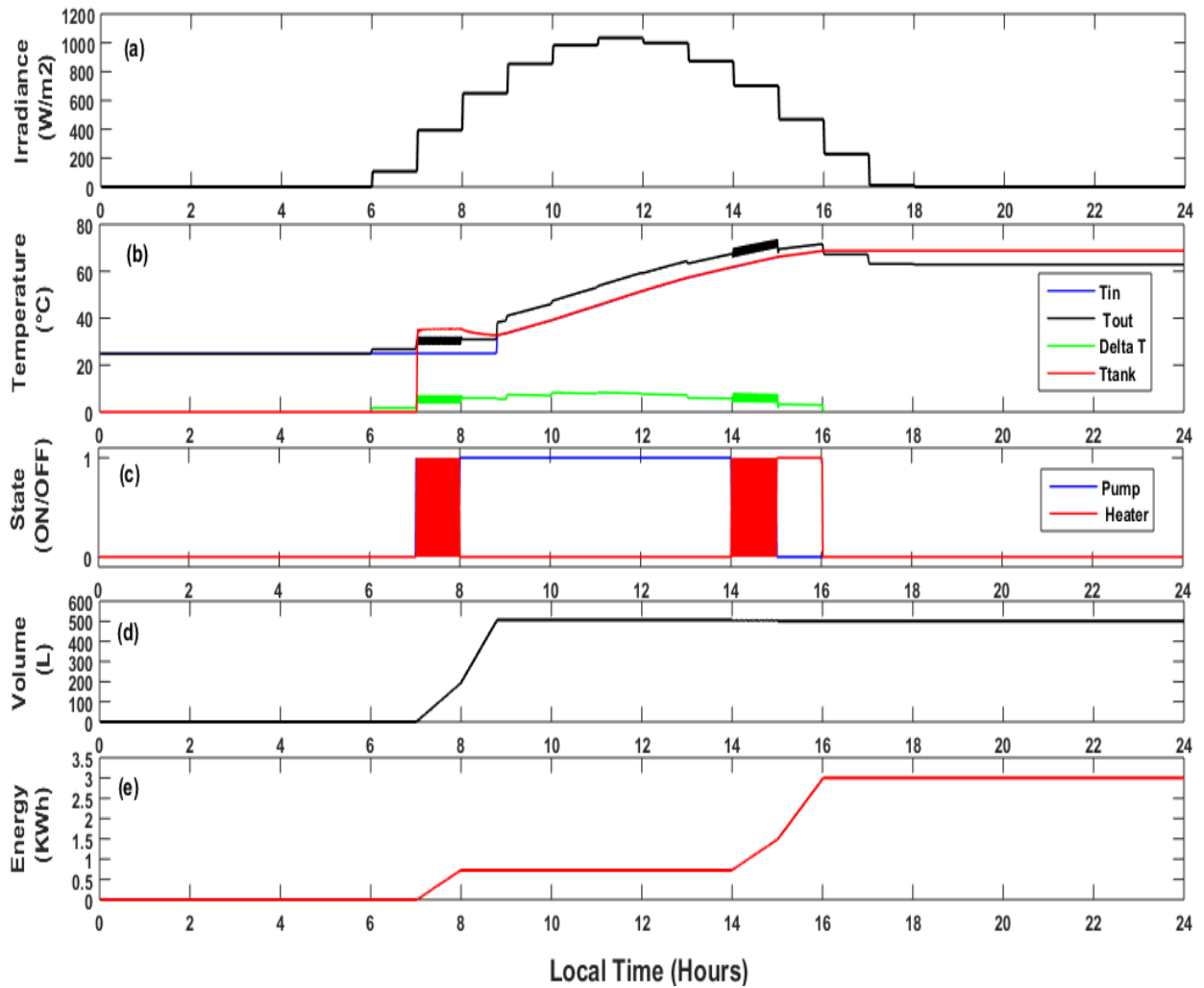


Fig. 7. As in figure 5 but with total panel’s surface of 5.5 m²

Though the need is still globally satisfied, an extra period of activity of the heater is noted (figure 7.c) after 3:30pm. This leads to reduction of the overall efficiency of the system since the total energy consumed by the electric heater has increased in this case to 3kWh. This tendency would be maintained if the surface is further reduced.

3.6. Impact of low solar radiation on the heating performances

In sizing the solar array, particular attention must be paid on the local meteorological conditions that may impact the

irradiance. Figure 8 shows the system performances with a 10% reduction in the incident solar radiation but a normal solar collector surface of 5.96 m². In this context, we observed that though the electric heater totally consumes 3kWh with an additional active period of the heater as noticed before, the final temperature of water in the tank is 67.36°, quite below the expected value. Therefore, a security coefficient that can vary with the locality may be applied to the sized total surface of the panels to take care of low solar radiation conditions.

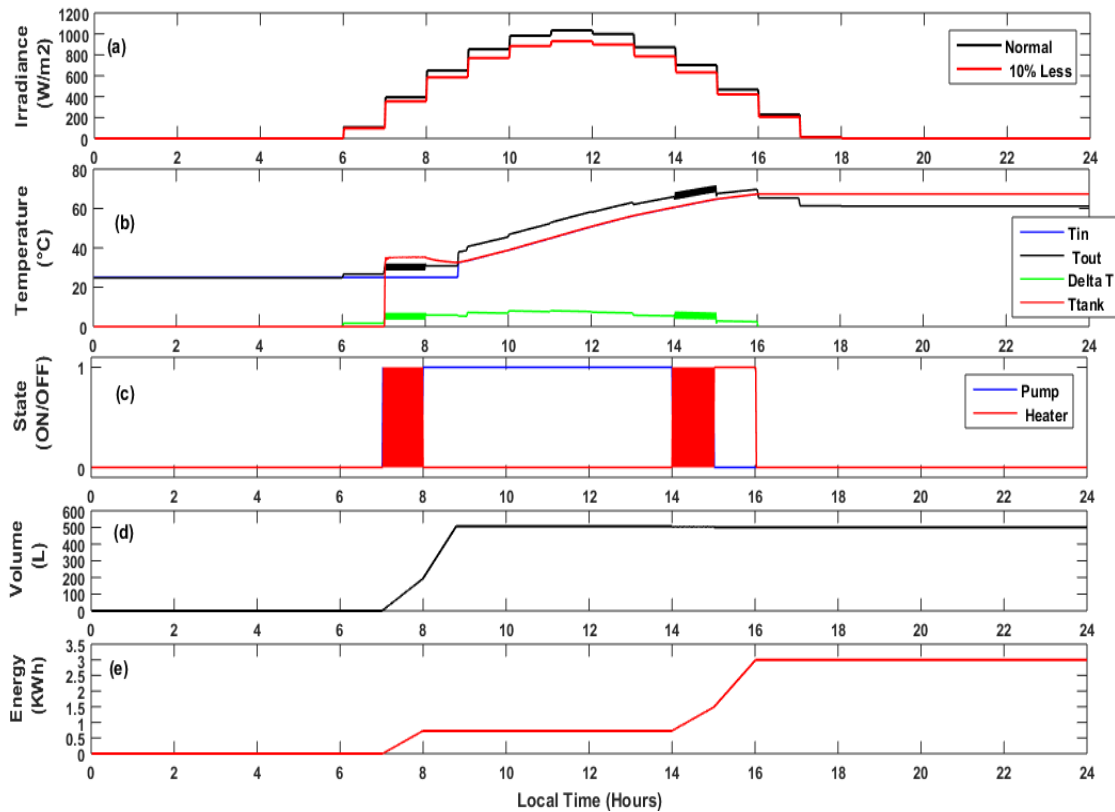


Fig. 8. System performance with 10% reduction in solar radiation.

4. Conclusion

This paper describes the complete design and control of an automatic active domestic solar water heating system (ADSWHS) in Wum using flat plate solar collectors. The daily hot water demand of 500L supplied at 70°C was required. To meet this load demand, 26.188 KWh of energy was required for the system. An efficient low-cost control strategy using water recirculation was achieved for the system using a microcontroller. The control system simulated results using hourly solar data for January obtained from PVGIS indicates that the system is able to produce the required daily hot water demand using solar thermal energy conversion that is clean and economically viable despite its high initial cost. The results further indicate that 6.59KWh of energy was used to run the pump and the auxiliary electric heater during this period while producing 26.188 KWh of clean energy to heat the water from 25°C to 70°C.

References

1. I. G. Kelechi, A. M. Zungeru, O. E. Ayobami, H. Habibu, A. F. Olugbenga, (2014), "Design and Modelling of a Solar Water Heating System". *Industrial Engineering Letters*, 4(12) 71
2. V. Msomi and O. Nemraoui, (2017), "Improvement of the Performance of solar water heater based on nanotechnology", 6th International Conference on renewable energy research and applications, San Diego, CA, USA
3. O. Bamisile, Akinola A. Babatunde, M. Dagbasi and I. Wole-Osho (2017), "Assessment of Solar Water Heating In Cyprus:Utility, Development and Policy", *International Journal of Renewable Energy Research*, 7(3), 1448-1453.
4. A. Harrouz, I. Daouali, K. Kayisli, H. I. Bulbul and I. Colak (2018), "Comparative Study between CSP and CPV as Two Energy Systems", 7thInternational Conference on Renewable Energy Research and Applications (ICRERA), PARIS, 1380-1383.
5. B. H. Abdulkadir and M. Muhammadu, (2012) "Design, construction and Performance Evaluation of a Solar Water Pump". *IOSR Journal of Engineering*, 2 (4), 711-718.
6. R. Li and Min Su, (2017). "The Role of Natural Gas and Renewable Energy in Curbing Carbon Emission: Case Study of the United States," *Sustainability*, MDPI, Open Access Journal, 9(4), 1-18.

7. M. H. Ahmed, A. Giaconia and A. M. A. Amin, (2017), "Effect of Solar Collector Type on the Absorption System Performance", 6th International Conference on Renewable Energy Research and Applications (ICRERA), San Diego, CA, 304- 309.
8. B. Ouhammou, M. Aggour, B. Daouchi (2018), Optimization of the Thermal Performance of the Solar Water Heater (SWH) Using Stochastic Technique, International Journal of Renewable Energy Research, 8(3).
9. Y. Yoshida and Y. Ueda, "Verification of consumer's benefits for different area ratio of PV array and solar thermal water heater considering regional characteristics," (2015) International Conference on Renewable Energy Research and Applications (ICRERA), Palermo, 472-477, doi: 10.1109/ICRERA.2015.7418457.
10. Y. Shimizu, T. Sakagami, and H. Kitano (2017), "Prediction of Weather Dependent Energy Consumption of Residential Housings" 6th International Conference on renewable energy research and applications, San Diego, CA, 967-970.
11. B. Greening, A. Azapagic, (2014), Domestic solar thermal water heating: A sustainable option for the UK, Renewable Energy 63, 23-36
12. H. I. Abu-Mulaweh, (2012), "Design and development of solar water heating system experimental apparatus", Global Journal of Engineering Education, 14(1), 99–105.
13. M. Z. H. Khan, M. R. Al-Mamun, S. Sikdar and P. K. Halder, (2016), "Design, Fabrication, and Efficiency Study of a Novel Solar Thermal Water Heating System Towards Sustainable Development" Hindawi Publishing Corporation International Journal of Photoenergy, 2016, Article ID 9698328, 8 pages <http://dx.doi.org/10.1155/2016/9698328>
14. S. A. Kalogirou, S. Karellas, K. Braimakis, C. Stanciu and V. Badescu, (2016), "Exergy analysis of solar thermal collectors and processes", Prog. Energy Combust. Sci. 56, 106–137.
15. M. E. A. Slimani, M. Amirat, S. Bahria, I. Kurucz, M. Aouli and R. Sellami, (2015), "Study and modeling of energy performance of a hybrid photovoltaic/thermal solar collector: Configuration suitable for an indirect solar dryer", Energy Convers. Manag., 125, 209 -221.
16. J. Assaf and B. Shabani, (2016) "Transient simulation modelling and energy performance of a standalone solar-hydrogen combined heat and power system integrated with solar-thermal collectors", Appl. Energy, 178(41), 66–77.
17. C. Serir, D. Rekioua, N. Mezzai and S. Bacha, (2016), "Supervisor control and optimization of multi-sources pumping system with battery storage", Int. J. Hydrogen Energy, 41(45), 20974–20986.
18. M. Beschi, F. Padula and A. Visioli, (2016), "Fractional robust PID control of a solar furnace", Control Eng. Pract., 56, 190–199.
19. M. Fatehnia, S. Paran, S. Kish and K. Tawfiq (2016), "Automating double ring infiltrometer with an Arduino microcontroller", Geoderma, 262, 133–139
20. Weather data for Wum, available at www.weatherbase.com. Accessed on 20 October 2019
21. P. J. Axaopoulos, E. D. Fylladitakis, (2014), "Photovoltaic engineering e-learning applications developed for remote laboratory experimentation systems". Int. J. Energy Environ. Eng. 5, 78(14).<https://doi.org/10.1007/s40095-014-0078-4>
22. S. A. Mousavi Maleki, H. Hizam and C. Gomes, (2017), Estimation of Hourly, Daily and Monthly Global Solar Radiation on Inclined Surfaces: Models Re-Visited". Energies, 2017, 10, 134.
23. Photovoltaic Geographical Information System (PVGIS) database for Africa, "Hourly solar irradiation in Wum for January" available at www.pvgis.net. Accessed on 10 February 2020
24. L. N. Akana and D. Njomo, (2020), "Optimization and Sizing of a Stand-Alone Photovoltaic System and Assessment of Random Load Fluctuation on Power Supply". Energy and Power Engineering, 12, 28-43.
25. I. A. Odigwe, O. O. Ologun, O.A. Olatokun, A. A. Awelewa, A.F. Agbetuyi and I.A. Samuel, (2013), "A microcontroller-based Active Solar Water Heating System for Domestic Applications", International Journal of renewable energy research., 3(4), 837-845
26. C. S. Malvi, A. Gupta, M.K. Guaur, (2016), "Experimental investigation of heat removal factor in solar flat plate collectors for various flow configurations", International Journal of Green Energy, 14(4), 44-448. ISSN 1543-5075.